

Optical Absorption of Small Palladium-Doped Gold Clusters

Kaydashev, Vladimir; Ferrari, Piero; Heard, Christopher; Janssens, Ewald; Johnston, Roy L.; Lievens, Peter

DOI:

[10.1002/ppsc.201600036](https://doi.org/10.1002/ppsc.201600036)

License:

None: All rights reserved

Document Version

Peer reviewed version

Citation for published version (Harvard):

Kaydashev, V, Ferrari, P, Heard, C, Janssens, E, Johnston, RL & Lievens, P 2016, 'Optical Absorption of Small Palladium-Doped Gold Clusters', *Particle & Particle Systems Characterization*, vol. 33, no. 7, pp. 364-372. <https://doi.org/10.1002/ppsc.201600036>

[Link to publication on Research at Birmingham portal](#)

Publisher Rights Statement:

This is the peer reviewed version of the following article: Kaydashev, V., Ferrari, P., Heard, C., Janssens, E., Johnston, R. L. and Lievens, P. (2016), Optical Absorption of Small Palladium-Doped Gold Clusters. Part. Part. Syst. Charact., 33: 364–372. , which has been published in final form at <http://dx.doi.org/10.1002/ppsc.201600036>. This article may be used for non-commercial purposes in accordance with Wiley Terms and Conditions for Self-Archiving.

Checked 21/7/2016

General rights

Unless a licence is specified above, all rights (including copyright and moral rights) in this document are retained by the authors and/or the copyright holders. The express permission of the copyright holder must be obtained for any use of this material other than for purposes permitted by law.

- Users may freely distribute the URL that is used to identify this publication.
- Users may download and/or print one copy of the publication from the University of Birmingham research portal for the purpose of private study or non-commercial research.
- User may use extracts from the document in line with the concept of 'fair dealing' under the Copyright, Designs and Patents Act 1988 (?)
- Users may not further distribute the material nor use it for the purposes of commercial gain.

Where a licence is displayed above, please note the terms and conditions of the licence govern your use of this document.

When citing, please reference the published version.

Take down policy

While the University of Birmingham exercises care and attention in making items available there are rare occasions when an item has been uploaded in error or has been deemed to be commercially or otherwise sensitive.

If you believe that this is the case for this document, please contact UBIRA@lists.bham.ac.uk providing details and we will remove access to the work immediately and investigate.

Particle and Particle Systems Characterization

Optical absorption of small palladium doped gold clusters

--Manuscript Draft--

Manuscript Number:	ppsc.201600036R1
Full Title:	Optical absorption of small palladium doped gold clusters
Article Type:	Full Paper
Section/Category:	Advanced Particle Characterization Techniques - invitation only
Keywords:	gold clusters; palladium doping; optical absorption
Corresponding Author:	Peter Lievens, Ph.D. KU Leuven Leuven, BELGIUM
Corresponding Author Secondary Information:	
Corresponding Author's Institution:	KU Leuven
Corresponding Author's Secondary Institution:	
First Author:	Vladimir Kaydashev, Ph.D.
First Author Secondary Information:	
Order of Authors:	Vladimir Kaydashev, Ph.D. Piero Ferrari Christopher Heard Ewald Janssens, Ph.D. Roy L. Johnston Peter Lievens, Ph.D.
Order of Authors Secondary Information:	
Abstract:	The effect of Pd doping on the structure and optical absorption of small cationic gold clusters is investigated by a combined photodissociation spectroscopy and time-dependent density functional theory study of Au_n+Arp and $PdAu_{n-1}+Arp$ ($n=4,5$; $p=0,1$). While pure Au clusters are planar, the Pd doped clusters are three dimensional. UV-visible absorption is studied in the 2.0-4.7 eV photon energy range, allowing the observation of previously unreported absorption bands for Au_4^+ and Au_4+Ar . The oscillator strength of the optical transitions is dramatically reduced upon incorporating a Pd atom in Au_4^+ and Au_4+Ar , while this effect is less pronounced for Au_5+Ar . Analysis of the electron density transfer shows a different influence of Pd with size. While Pd has a formal negative charge in Au_3Pd^+ , in Au_4Pd^+ most of the charge is attracted by the highly coordinated central Au atom, leaving Pd positively charged, also affecting the induced structural changes. In addition, orbital analysis of the optical transitions was carried out in order to identify the levels involved in the optical absorption of the pure Au and Pd doped clusters. A reduction of the s density near the Fermi energy, induced by Pd doping, causes a quenching of optical absorption.
Additional Information:	
Question	Response
Please submit a plain text version of your cover letter here.	Dear editors
Please note, if you are submitting a revision of your manuscript, there is an opportunity for you to provide your responses to the reviewers later; please	Herewith we submit our manuscript entitled: "Optical absorption of small palladium doped gold clusters" as a paper for the special issue on "Advanced Particle Characterization Techniques", upon invitation by prof. Sara Bals and prof. Luis M. Liz-Marzán.

do not add them to the cover letter.

The paper deals with a combined experimental and theoretical study of the optical properties of small gold clusters and how these properties are influenced by chemical and structural changes upon doping with a single Pd atom. The experimental work essentially is based on mass spectrometry and action spectroscopy, and the theoretical work uses density functional theory.

Our findings clearly demonstrate the importance of structural changes on the electronic structure, and hence the optical properties, in such small particles. The detailed investigation reveals that charge distribution, different for different investigated sizes and compositions, plays an important role. Another observation is the strong quenching of optical absorption upon doping gold clusters with palladium. While this was investigated experimentally before, this study combined with theory revealed that this is related to the altered electronic states, in particular the significant reduction of s-d mixing when a palladium atom is incorporated.

We do hope that this study on very small clusters provides an interesting and broadening contribution to the special issue of Particle, in the limit of very small particles.

On behalf of the co-authors,
Peter Lievens

1 DOI: 10.1002/ppsc.((please add manuscript number))

2 **Article type: Full paper**

3
4
5 **Optical absorption of small palladium doped gold clusters**

6
7
8 *Vladimir Kaydashev, Piero Ferrari, Christopher Heard, Ewald Janssens*, Roy L. Johnston,*
9 *and Peter Lievens*

10
11
12
13 Dr. V. Kaydashev, P. Ferrari, Prof. Dr. E. Janssens, Prof. Dr. P. Lievens
14 Laboratory of Solid State Physics and Magnetism, KU Leuven, 3001 Leuven, Belgium
15 E-mail: ewald.janssens@fys.kuleuven.be

16 Dr. C. Heard

17 Department of Applied Physics, Chalmers University of Technology, Gothenburg, Sweden

18 Prof. Dr. R. L. Johnston

19 School of Chemistry, University of Birmingham, Edgbaston, Birmingham B15 2TT, UK
20
21
22
23

24 **Keywords:** gold clusters, palladium doping, optical absorption

25
26
27 The effect of Pd doping on the structure and optical absorption of small cationic gold clusters
28 is investigated by a combined photodissociation spectroscopy and time-dependent density
29 functional theory study of Au_n^+Ar_p and $\text{PdAu}_{n-1}^+\text{Ar}_p$ ($n=4,5$; $p=0,1$). While pure Au clusters
30 are planar, the Pd doped clusters are three dimensional. UV-visible absorption is studied in
31 the 2.0–4.7 eV photon energy range, allowing the observation of previously unreported
32 absorption bands for Au_4^+ and Au_4^+Ar . The oscillator strength of the optical transitions is
33 dramatically reduced upon incorporating a Pd atom in Au_4^+ and Au_4^+Ar , while this effect is
34 less pronounced for Au_5^+Ar . Analysis of the electron density transfer shows a different
35 influence of Pd with size. While Pd has a formal negative charge in Au_3Pd^+ , in Au_4Pd^+ most
36 of the charge is attracted by the highly coordinated central Au atom, leaving Pd positively
37 charged, also affecting the induced structural changes. In addition, orbital analysis of the
38 optical transitions was carried out in order to identify the levels involved in the optical
39 absorption of the pure Au and Pd doped clusters. A reduction of the s density near the Fermi
40 energy, induced by Pd doping, causes a quenching of optical absorption.
41
42
43
44
45
46
47
48
49
50
51
52
53
54
55
56
57
58
59
60
61
62
63
64
65

1. Introduction

The unique characteristics of gold clusters and nanoparticles have received significant attention in recent decades. In particular, their optical properties and chemical reactivities are used in the design of novel environmental applications, including photo-catalytic water splitting,^[1] CO oxidation,^[2] molecular hydrogen dissociation^[3] and the design of efficient solar cells.^[4] To enhance understanding, small unsupported atomic clusters, consisting of only a few atoms, represent ideal model systems for detailed investigations.^[5] Moreover, many properties of small atomic clusters do not scale with size, are strongly composition and charge dependent, and can be very different from those of bulk materials.^[6] Research on clusters in the gas phase can be performed under controlled conditions and without interactions with the environment, thus providing fundamental knowledge of relevance for the understanding of more complex systems.^[7]

Structural and ground state electronic properties of small Au clusters in different charge states have been largely characterized.^[8-12] In addition, significant efforts have been made concerning the investigation of optical properties of clusters. Studies on mass selected clusters, e.g. Cu_n, Ag_n and Au_n have been performed in rare gas (RG) matrices,^[13-16] because direct optical measurements are challenging and require advanced techniques.^[17] This is a consequence of the very low density of clusters in molecular beams. Although experiments on embedded clusters in RG matrices have been successful, a drawback of this approach is that weak interactions with the rare gas matrix must be considered. An alternative is presented by photodissociation spectroscopy.^[18] In this technique, laser light absorption is monitored mass spectrometrically via photon induced fragmentation, rather than by changes in light intensity. Using this method, UV-visible optical absorption was studied for several mass selected Au, Ag, and Cu clusters: Au₄⁺Ar_p (p = 0–4),^[19] Au_n⁺Ar_p (n = 7; p = 0–3 and n = 8, 9; p = 0, 1),^[20] Au_n⁻Xe (n = 7–11),^[21] Ag₄⁺ and Au₄⁺,^[22] Ag_n⁺ (n = 6, 8),^[23] and Cu₃.^[24] An important

Particle

Submitted to **& Particle Systems Characterization**

1 observation from these experiments is the rather complicated absorption features of Au
2 clusters in contrast with Cu and Ag coinage metal clusters.^[22] The heavy Au atoms are subject
3 to significant relativistic effects resulting in a reduced valence s-d energy separation partially
4 involving d-electrons in the absorption process.^[25] Close-lying d electrons screen s electrons
5 and thereby reduce the optical absorption bands. In contrast, the larger s-d separation in Ag
6 allows the use of free electron models to describe its optical response, such as the plasmonic-
7 like absorption spectra of very small Ag_n^+ ($n = 4, 6, 8$) clusters.^[22, 23]

8 The properties of coinage metal clusters can be tuned by dopant atoms.^[26] It has been shown
9 that the addition of a single dopant atom can drastically change the stability,^[27] reactivity,^[28]
10 and electronic properties of clusters.^[29] In addition it is expected that the optical absorption of
11 coinage metal clusters should also be drastically affected by the inclusion of dopant atoms.
12 However, so far only a few experimental studies have dealt with this problem. In the 1990s,
13 Morse and co-workers studied AgAu and CuAu dimers.^[30,31] More recently, optical
14 absorption measurements were carried out for $\text{Au}_{4-m}\text{Cu}_m^+$ ($m = 0-2$)^[32] and $\text{Ag}_n\text{Au}_{4-n}^+$ ($n = 1-$
15 3) clusters in the gas phase.^[33]

16 Of particular interest are Pd doped Au clusters. Bonding between Au and Pd atoms involves
17 promotion of at least one Pd 4d electron to a 5s orbital and thus, significant charge
18 redistribution takes place.^[34] These modifications of the electronic structure can, for instance,
19 enhance the chemical reactivity of Au towards CO and O₂ in Au_nPd ($n \leq 7$) or lead to Pd
20 dopant induced 2D to 3D structural transitions due to the orbital orientations provided by
21 Pd.^[35,36] Using DFT calculations, low energy structures of Pd doped gold clusters of different
22 sizes and charge states have been predicted: Au_nPd^m ($n = 1-4, m = -1, 0, 1$),^[36] Au_nPd_m ($n+m \leq$
23 14),^[37] Au_nM ($n = 1-7, M = \text{Ni, Pd, Pt}$),^[29] Au_nPd ($n = 1-4$),^[38] and $\text{Au}_{32-m}\text{Pd}_m$ ($m = 1, 2, 4,$
24 6).^[39]

1 It has been shown that also the properties of larger Au nanoparticles (2-5 nm) can be
2 significantly modified by introduction of other metals. In particular, in the Au-Pd alloy
3 nanoparticles an increased d-electron density at the Au sites was observed by XANES
4 experiments, giving rise to a Au “white” line intensity decrease and decreasing Au 4f binding
5 energies in XPS studies, evidencing the charge transfer from Pd to Au 5d orbitals.^[40,41] The
6 effect is higher when the number of Au-Pd bond increases.
7

8 Recently, some of us experimentally investigated the effect of Pd on the optical absorption of
9 Au_n⁺ (13 ≤ n ≤ 20) clusters.^[42] A strong quenching effect of the absorption bands upon Pd
10 doping was observed for all studied sizes, though with a noticeable size dependent alteration,
11 and was attributed to dopant induced charge redistribution. In order to determine whether
12 these effects extend down to the smallest clusters, in the current work, we investigate the
13 effect of Pd on the optical absorption properties of Au₄⁺, Au₄⁺Ar and Au₅⁺Ar clusters in a
14 broad photon energy range of 2.0–4.7 eV, using a combined photodissociation spectroscopy
15 and time-dependent density functional theory (TDDFT) approach. The calculations provide
16 understanding of the effect of the Pd dopant on optical properties and the interplay between
17 electronic structure and optical absorption.
18
19
20
21
22
23
24
25
26
27
28
29
30
31
32
33
34
35
36
37
38
39
40

41 **2. Methods**

42 **2.1. Experimental setup and data analysis**

43 Cationic pure gold and Pd-doped gold clusters are simultaneously produced in a dual-target
44 dual-laser vaporization source.^[43] The second harmonic of two independent Nd:YAG pulsed
45 lasers (532 nm, 10 Hz) is used to ablate separately Au and Pd targets. Just before ablation, a
46 small amount of He gas is introduced at 8 bar by a supersonic valve, thermalizing the ablated
47 plasma via heat exchange between the carrier gas and the source walls, which are cooled by a
48 constant flow of liquid nitrogen. Using a temperature controller, the source can be stabilized
49 to any temperature in the range of 80–300 K. In this study a source temperature of 250 K is
50
51
52
53
54
55
56
57
58
59
60
61
62
63
64
65

1 selected. A small concentration of Ar (2%) is added to the carrier gas to form cluster–Ar
2
3 complexes.^[44] After expansion into vacuum through a conical nozzle, the central part of the
4
5 beam is selected by a skimmer and clusters enter the extraction region of a reflectron time-of-
6
7 flight (TOF) mass spectrometer. Total fraction of Ar complexes for Au_n⁺ and PdAu_{n-1}⁺ (n=1-
8
9 13) clusters observed in mass spectra is available in **Figure S1** of the Supporting Information.
10
11 To measure photodissociation spectra of bare clusters and their Ar complexes, the particles
12
13 are excited in the extraction zone of the TOF by laser light. Tunable lasers were employed to
14
15 cover the entire 2.0 to 4.7 eV photon energy range. For the 262–340 nm and 370–620 nm
16
17 ranges a Nd:YAG pumped optical parametric oscillator (Quanta-Ray, MOPO-710, 10 Hz)
18
19 with a BBO-crystal based frequency doubling unit (Quanta-Ray FDO-1) was used, while the
20
21 340–370 nm range was covered by a Nd:YAG pumped dye laser (Sirah Cobra Stretch, 10 Hz)
22
23 using Pyridine 1, Pyridine 2 and Styryl 8 as dyes and a KDP crystal for second harmonic
24
25 generation. The energy per pulse is monitored by a pyroelectric energy sensor (ThorLabs,
26
27 ES111C) and maintained below 5 mJ/cm² per pulse to avoid two-photon processes. Using a
28
29 chopper, operated at 5 Hz and synchronized with the tunable lasers, mass spectra with and
30
31 without laser excitation are recorded simultaneously. Each mass spectrum is an average of
32
33 over 5000 cluster production cycles.
34
35
36
37
38
39
40
41

42 Photodepletion is measured as a function of photon energy and is defined as the ratio of the
43
44 intensities of a certain species in the mass spectra recorded with (*I*) and without (*I*₀) laser
45
46 excitation. Then, this ratio is converted into absorption cross section using the modified
47
48 Lambert-Beer-Law:^[19]
49

$$50 \quad I/I_0 = 1 - b + b \exp(-\sigma\Phi), \quad (1)$$

51
52 where Φ is the photon fluence, σ the absorption cross section and b a factor taking into
53
54 account an imperfect spatial and temporal overlap between dissociation laser and extracted
55
56 clusters. It is worth stressing that Equation 1 assumes only one-photon processes are
57
58
59
60
61
62
63
64
65

1 responsible for absorption.^[21] From fluence dependence curves an overlap factor b of 0.5 is
2
3 estimated (**Figure S2** of Supporting Information).
4
5
6

7 **2.2. Computational details**

8
9 The density functional theory genetic algorithm (GA-DFT) global optimization approach is
10 utilized to locate the global minimum structures of the metallic clusters, along with several
11 energetically low-lying local minima. This approach involves the coupling of the unbiased
12 structure prediction code, the Birmingham Cluster Genetic Algorithm (BCGA), to the plane-
13 wave DFT electronic structure calculation package Quantum Espresso (QE).^[45,46] DFT
14 screening of cluster structures is performed with the PBE exchange-correlation functional,
15 within the spin-unrestricted, generalized gradient DFT framework.^[47] For Au and Pd atoms,
16 11 and 10 electrons are explicitly included in the valence, respectively, with the effect of all
17 remaining electrons represented by ultrasoft RRKJ pseudopotentials.^[48] Individual cluster
18 convergence is achieved according to a force cutoff of 10^{-2} eV/Å and electronic self-
19 consistency of 10^{-5} eV. Upon convergence of the BCGA, the final generation of structural
20 candidates are subjected to geometry reoptimization within the NWCHEM v6.1 package.^[49]
21 This orbital-based method is applied with an extensive 19-electron def2-TZVPP basis set for
22 all atoms and the corresponding effective core potential (def2-ECP) of Weigend and Ahlrichs
23 is additionally employed for Au and Pd atoms.^[50] The range-separated exchange-correlation
24 functional LC- ω PBEh is used,^[51,52] due to its recently proven good performance for the
25 structures and optical spectra of Au and AuAg clusters in this size range.^[22,33] After local
26 reoptimization, a frequency analysis is performed for all putative global minima to verify that
27 each is a true minimum structure. Argon tagging is performed for each global minimum
28 metallic cluster structure, considering all symmetry-inequivalent sites and subsequently
29 optimizing local geometry.
30
31
32
33
34
35
36
37
38
39
40
41
42
43
44
45
46
47
48
49
50
51
52
53
54
55
56
57
58
59
60
61
62
63
64
65

1 For minimum-energy structures resulting from the DFT optimizations, electronic excitation
2
3 spectra are calculated using spin-unrestricted TDDFT considering 60 excited states. All
4
5 excited state calculations are performed with NWChem, using the same exchange–correlation
6
7 functional and basis set as in the geometry optimization step.^[50] The output from optical
8
9 response calculations is analyzed using Chemissian, an analytical tool for electronic structure
10
11 and spectra calculations.^[53]
12
13
14
15
16
17

18 **3. Results**

19 **3.1. Fragmentation channels and dissociation energies**

20 Examples of typical mass spectra with (black) and without (red) laser excitation are presented
21
22 in **Figure 1**. As seen from Figure 1a and 1b, Au_4^+ and Au_4^+Ar shows signal depletion under
23
24 laser excitation at wavelengths of 482 and 460 nm, respectively. The situation, however, is
25
26 different for Au_3^+ (Figure 1a and 1b), showing a considerable signal increase. Several most
27
28 probable fragmentation channels were assumed analysing the behaviour of mass spectra. In
29
30 order to understand the clusters fragmentation behaviour under photoabsorption the lowest
31
32 energy fragmentation channels of Au_n^+Ar_m ($n = 4, 5$; $m = 0, 1$) and $\text{PdAu}_{n-1}^+\text{Ar}_m$ ($n = 4, 5$; m
33
34 $= 0, 1$) clusters were calculated by DFT simulations and analysed together with observations.
35
36
37
38
39
40

41 A list of channels and dissociation energies is presented in **Table 1**.

42
43 Fragmentation of Au_4^+ occurs by monomer evaporation. The calculated dissociation energy
44
45 for this channel (1.33 eV) is well below the single photon energy of the experimentally
46
47 investigated spectral range (2.0–4.7 eV). This result is supported by the measurements
48
49 presented in Figure 1a and 1b, in which Au_4^+ depletion coincides with Au_3^+ signal increase, as
50
51 also seen in previous experiments.^[19,22,32] PdAu_3^+ preferentially dissociates by loss of a
52
53 neutral Au atom, but the calculated dissociation energy (2.25 eV) is much larger and is higher
54
55 than the lowest photon energy used. This should be considered when interpreting the optical
56
57 absorption spectra, since bands are only observed in action spectroscopy if the single photon
58
59
60
61
62
63
64
65

1 absorptions finally results in cluster fragmentation. For photon energies that are only slightly
2
3 higher than the energy needed for dissociation, the cluster fragmentation may occur at time
4
5 scales longer than those of the experiment.^[54] The investigation of cluster–Ar complexes is
6
7 relevant in this context since the cluster–Ar bond is weak and will break rapidly following
8
9 adsorption of a single UV or visible photon. This is confirmed by the calculated Ar
10
11 evaporation energies that are of the order of 0.2 eV only (Table 1), in agreement with
12
13 previous calculations.^[55] Actually the experiments show that the absorption of a photon by the
14
15 Au_4^+Ar cluster leads to simultaneous evaporation of an Ar and a Au atom, as shown in Figure
16
17 1b. This is consistent with the low calculated energy required for this process (1.54 eV).
18
19

20
21
22 In contrast to Au_4^+ , the lowest energy fragmentation channel of Au_5^+ is found to be dimer
23
24 evaporation, with a dissociation energy of 2.17 eV. Monomer evaporation from this cluster
25
26 leads to a dissociation energy of 2.74 eV, much larger than for dimer evaporation. The case of
27
28 PdAu_4^+ , however, is different. The dissociation energy of monomer evaporation is found
29
30 lower, being 1.64 eV, while for dimer evaporation the larger value of 2.07 eV is obtained.
31
32

33
34 Finally, it is worth to mention that for the applied experimental conditions multiple Ar
35
36 complexes are formed for Au_5^+ : Au_5^+Ar_m with $m = 1-3$, as shown in **Figure S3** of the
37
38 Supporting Information. The depletion spectrum of Au_5^+Ar may be contaminated by
39
40 fragmentation of Au_5^+Ar_2 and Au_5^+Ar_3 , although the data suggest that all Ar atoms are
41
42 evaporated simultaneously following photon adsorption and such contamination is therefore
43
44 likely to be limited.
45
46
47
48
49
50

51 **3.2. Optical absorption of Au_4^+ and PdAu_3^+ clusters**

52
53 The calculated absorption spectra of Au_4^+ and PdAu_3^+ are compared with the experimental
54
55 photodissociation spectra in **Figure 2**. Photon absorption cross sections are calculated as a
56
57 function of excitation energy from the measured photodepletions using Equation 1. **The**
58
59 **photodepletion curves only show signal decrease, implying that the measured spectra for Au_4^+**
60
61
62

Particle

Submitted to *& Particle Systems Characterization*

1 and PdAu₃⁺ are not contaminated by fragmentation of larger clusters. Indeed, calculated
2
3 fragmentation pathways (Table 1) indicate that Au₄⁺ is neither the preferred fragment of Au₅⁺
4
5 nor of Au₄⁺Ar, since Au₅⁺ favors dimer evaporation and Au₄⁺Ar evaporates simultaneously Ar
6
7 and Au after photoexcitation in the measured spectral range. On the other hand,
8
9 photodissociation of PdAu₄⁺ may produce PdAu₃⁺, but this process seems not to be likely,
10
11 since no contamination observed in the spectra of PdAu₃⁺. Due to the noise level of the
12
13 measurements, features with cross sections below 0.25 Å² are not labeled as bands. As a
14
15 standard procedure, data were averaged by 3-adjacent points in order to identify absorption
16
17 features and then, based on this average, a multi-Gaussian fit was applied to the raw data.
18
19 Using this criterion, four resonant excitations are observed for Au₄⁺, with maxima at 2.58 eV
20
21 (A), 3.49 eV (B), 3.87 eV (C) and 4.43 eV (D). Of these four bands, feature B at 3.49 eV is
22
23 clearly the most intense. Previous gas phase studies of Au₄⁺ were performed with photon
24
25 energies below 3.5 eV and hence only reported band A at 2.58 eV,^[19,20,22,32] and an onset of
26
27 band B.^[22] UV-visible absorption measurements of neutral mass selected gold clusters
28
29 embedded in Ne matrices were carried out in the extended energy range of 1.5-6.0 eV,
30
31 showing a strong absorption feature at 3.17 eV, close to band B.^[16]
32
33
34
35
36
37
38
39 In order to isolate the electronic properties of the optical spectra, TDDFT calculations were
40
41 performed on the energetically lowest-lying isomers as calculated with DFT. Figure 2b shows
42
43 that the computed spectrum, calculated with the rhombic minimum energy structure of Au₄⁺
44
45 shown as inset, is in good agreement with the experiment if a redshift of the computed bands
46
47 B, C, and D of about 0.2 eV is taken into account.^[19,22,32] In Ref. [22], the simulated peak at
48
49 3.3 eV was assigned to a low intensity band at 3.2 eV, and the existence of an experimental
50
51 band at 3.5 eV was interpreted as the presence of additional isomers in the beam. In the
52
53 current work, we suggest that the calculated peak B may be a redshifted representation of the
54
55 experimental peak B. For all peaks above 3.0 eV, both in the current work and in Ref. [22],
56
57
58
59
60
61
62
63
64
65

1 the transitions are of the same type, primarily Au 5d to Au 6s interband transitions. The
2
3 computed band E at 4.42 eV is not observed experimentally. However, considering the
4
5 observed redshift of the calculated bands, feature E may be present at higher energies than
6
7 those measured.
8
9

10 The effect of substitution of Pd for Au in Au₄⁺ is significant. Structurally, the Pd dopant
11
12 induces a 2D → 3D transition similar to earlier calculations.^[34] As commented in the
13
14 introduction, the structural change is likely affected by the charge transfer expected upon Pd
15
16 doping. More surprising is the completely altered optical response. Using the earlier presented
17
18 criterion to identify signals with cross sections above 0.25 Å² as bands, only at the highest
19
20 photon energies (>4.6 eV) is the onset of a band found in the experimental spectrum of
21
22 PdAu₃⁺ (Figure 2c). The calculated spectrum, shown in Figure 2d, agrees well with the
23
24 experiment. Optical absorption bands are strongly suppressed, showing only an intense
25
26 feature at 4.56 eV, probably corresponding to feature A observed experimentally (again
27
28 considering a redshift of the computed spectrum relative to the experiment). Computations
29
30 also predict a signal at 2.3 eV, which may be sufficiently intense to be measurable. However,
31
32 the large dissociation energy calculated for PdAu₃⁺ (2.25 eV) likely suppresses fragmentation
33
34 following photoabsorption at low excitation energies, explaining the absence of that band in
35
36 Figure 2c.
37
38
39
40
41
42
43

44 Oscillator strengths, extracted from the measured absorption cross sections, are listed in
45
46 **Table 2** and compared with the calculated results.
47
48
49
50
51

52 **3.3. Optical absorption of Au₄⁺Ar and Au₃Pd⁺Ar clusters**

53 **Figure 3** presents the experimental photodissociation and calculated optical excitation spectra
54
55 of Au₄⁺Ar and PdAu₃⁺Ar. **In view of the dissociation energies listed in Table 1, it seems that**
56
57 **complexes with multiple Ar atoms loose the messenger atoms simultaneously upon**
58
59 **photoexcitation. So possible contamination of the spectra of Au₄⁺Ar and PdAu₃⁺Ar by**
60
61
62
63
64
65

dissociation of complexes with multiple Ar atoms is unlikely. Indeed, the photodissociation spectra show only signal decrease, which supports this assumption. Five bands, at energies 2.71 eV, 3.15 eV, 3.48 eV, 3.67 eV and 3.87 eV, can be distinguished in the experimental spectrum of Au_4^+Ar (Figure 3a). However, the rather high level of noise makes a clear distinction difficult. Comparing bands A of Au_4^+ (Figure 2a) and Au_4^+Ar , a blue shift of 0.1 eV is observed, as reported in previous studies.^[19, 32] Band B at 3.15 eV has also been observed previously.^[19] All bands above 3.4 eV are reported for the first time. The agreement with the calculated spectrum (Figure 3b) is fairly good, with minor energy shifts. The experimentally assigned bands D and E are not reproduced theoretically, which may be caused by not completely reliable band assignment in the experiment due to the low signal-to-noise level. However, another possibility is the coexistence of low-energy isomers in the beam. For this purpose the optical absorption spectrum of a y-shaped isomer was calculated and shown in blue dashed line in Figure 3b. This isomer, when Ar tagged, only is only 0.11 eV higher in energy than the global minimum and thus, could be present in the experiment. The y-shaped isomer has electronic excited states at 3.78 eV and 3.95 eV, close to the missing peaks in the experimental spectrum. All peaks for the calculated spectrum in this energy range are predominantly Au 5d – Au 6s or Au sd – Au 6s hybrid transitions.

As for the bare Au_4^+ and Au_3Pd^+ clusters, Pd doping quenches the optical absorption of the Ar complexes. Although the level of noise in the photodissociation spectrum of PdAu_3^+Ar hampers definitive band assignment, features A and B of Au_4^+Ar are clearly suppressed. This observation agrees well with the calculated absorption spectrum of PdAu_3^+Ar , with only two weak absorption bands at 3.70 eV and 4.44 eV.

3.4. Optical absorption of Au_5^+Ar and $\text{Au}_4\text{Pd}^+\text{Ar}$ clusters

In contrast to the photoexcitation of Au_4^+ , the Au_5^+ signal in the mass spectrum shows no depletion, but only signal increase, implying that its depletion spectrum is contaminated by

1
2
3
4
5
6
7
8
9
10
11
12
13
14
15
16
17
18
19
20
21
22
23
24
25
26
27
28
29
30
31
32
33
34
35
36
37
38
39
40
41
42
43
44
45
46
47
48
49
50
51
52
53
54
55
56
57
58
59
60
61
62
63
64
65

1 larger clusters dissociating into Au_5^+ . Therefore, only Ar complexes of Au_5^+ and Au_4Pd^+ are
2
3 discussed here. For these species the cluster- Ar_m complex peaks are depleted while the
4
5 intensity of the corresponding cluster without Ar increases. As Ar atoms are weakly bound by
6
7 Van der Waals forces with energy of ~ 0.2 eV (see Table 1) these typical action spectroscopy
8
9 channels are indeed very probable.
10

11 **Figure 4** displays experimental photodissociation and calculated absorption spectra for
12
13 Au_5^+Ar and PdAu_4^+Ar . Again the Pd dopant induces a 2D to 3D structural transition, but for
14
15 this cluster size the influence of the Pd dopant on the optical absorption spectrum is less
16
17 pronounced. Both Au_5^+Ar (Figure 4a) and PdAu_4^+Ar (Figure 4c) have an absorption feature at
18
19 around 3.5 eV (band A) and no appreciable quenching upon Pd-doping is observed for this
20
21 band. In addition, broad absorption features are observed for Au_5^+Ar above 4.0 eV, which are
22
23 somewhat reduced in intensity by Pd doping. Calculated absorption spectra, presented in
24
25 Figure 4b and 4d, show less agreement with the experiment. Calculated optical absorption of
26
27 multiple Ar complexes Au_5^+Ar_p ($p=1-3$) are available in Figure S5b of the Supporting
28
29 Information. Band A is reproduced in both clusters and it is blue shifted by about 0.4 eV for
30
31 Au_5^+Ar . For this cluster, two bands at 4.1 eV and 4.3 eV may represent the broad increase
32
33 observed experimentally in that range, in addition to a very intense band, at 4.5 eV, calculated
34
35 but not observed in the experiment. Nonetheless, this intense feature may occur at photon
36
37 energies above the investigated range. Calculated features between 3.8 eV and 4.4 eV for
38
39 PdAu_4^+Ar cannot be distinguished from the noise level experimentally.
40
41

42
43 Although the agreement between experiment and theory is better for the tetramers than the
44
45 pentamers, the different influence of Pd-doping on the optical spectra for the tetramers and
46
47 pentamers is in line with the induced structural changes.
48
49

50 4. Discussion

51 4.1. Structures and charge transfers

Particle

Submitted to **& Particle Systems Characterization**

1 As shown in Figure 2, 3 and 4, the structures of the Au_n^+ ($n = 4, 5$) clusters are affected by Pd-
2
3 doping. It is known that cationic Au clusters remain planar up to $n = 7$ while cationic pure Pd
4
5 clusters form 3D structures from $n = 4$ onwards.^[8,56] The relativistically enhanced s-d
6
7 hybridisation in gold causes an unusually large cluster size for the 2D-3D transition, as the
8
9 preferential overlap of valence orbitals which minimises electronic energy is in an in-plane
10
11 direction. This stabilisation is not present in palladium, and leads to compact, pseudospherical
12
13 structures.^[54] Thus, doping palladium atoms into gold clusters disrupts this planarity
14
15 stabilisation, and drives a transformation of dimensionality from 2D to 3D. We observe, in
16
17 agreement with previous studies, that this transition occurs as the smallest possible cluster
18
19 size of Au_nPd_m ($n+m=4$).^[29,58,59]

24
25 This 2D to 3D geometry change possibly diminishes the absorption cross section and is
26
27 therefore partially responsible for the overall absorption quenching accompanying Pd-doping.
28
29 A similar theoretical prediction of a decrease in cluster polarizability with changing Ag_n
30
31 structure from planar to three-dimensional at $n = 7$ has been discussed previously.^[60]

34
35 To analyse the charge transfer in more detail, electron densities are calculated. The results
36
37 according to the Löwdin scheme are presented in **Figure 5** and **Figure S4** of Supporting
38
39 Information. The positive charge in Au_4^+ is roughly equally distributed over the Au atoms.
40
41 Upon doping, Pd draws electron density from the Au atoms, which gives Pd a formal negative
42
43 charge in PdAu_3^+ . In Au_5^+ , however, due to its high symmetry, the central Au atom has zero
44
45 net positive charge and in PdAu_4^+ the central Au atom draws most of the charge, reducing the
46
47 charge available to the Pd atom, and hence its influence on the cluster's electronic properties.
48
49 In fact, even though PdAu_4^+ has a 3D structure, the average bond length between Au atoms in
50
51 the cluster is not notably affected by the Pd dopant, being 2.63 \AA for both PdAu_4^+ and Au_5^+ .
52
53 This situation is different for Au_4^+ and PdAu_3^+ , with average Au–Au distances of 2.66 \AA and
54
55
56
57
58
59
60
61
62

2.72 Å, respectively. An overview of the calculated average bond distances is available in **Table S1** of the Supporting Information.

4.2. Orbital analysis of optical transitions

4.2.1 Au_4^+ and $PdAu_3^+$ clusters

The suppression of the optical response on Pd doping is investigated by calculation of the states that make up the relevant region of the band structure. In **Figure 6**, a representative electronic correlation diagram is shown for Au_4^+ , $PdAu_3^+$, and Pd_4^+ . For the case of Pd_4^+ , the lowest energy structure is calculated as a Jahn-Teller distorted tetrahedron, with bonds of 2.72 Å in the basal plane, and a compressed z direction with bonds of 2.64 Å to the top atom.

The Au_4^+ cluster shows a significant degree of s-d mixing, which is primarily manifested at the top (0 eV) and bottom (-4.8 eV) of the d band, as well as in intermediate peaks throughout the band. The bands are molecular, due to the small size of the cluster, and thus molecular charge-transfer transitions, which result from the differences in electronic structure between non-equivalent atoms, may be resolved. One example is the s-d \rightarrow s-d transition from a hinge atom (0 eV) to the wingtip atom at +0.1 eV. For the Pd_4^+ cluster, the s-d mixing is diminished. The HOMO state is of 100% d character, and the first filled s state is at -1.5 eV. Therefore, interband s \rightarrow d and d \rightarrow s transitions, as well as intraband s \rightarrow s transitions are likely to be suppressed in Pd clusters. The doped $PdAu_3^+$ cluster represents an intermediate case, in which the width of the d band is between that of Au_4^+ and Pd_4^+ , and some s-d mixing is present due to the Au atoms. The first filled s state is at -0.9 eV, which lies between the values for the two monoelemental clusters, and represents a significant increase in energy required for optical transitions from s states as compared to Au_4^+ . The energy gap to s-like conduction band states is similarly increased, from 1.1 eV in Au_4^+ to 1.8 eV in $PdAu_3^+$. This overall depletion of s density near the Fermi energy is likely a major cause for the suppression of the optical absorption bands.

4.2.2 Au_4^+Ar and $PdAu_3^+Ar$ clusters

Upon Pd doping, the electronic character of the calculated transitions of $PdAu_3^+Ar$ is changed significantly with respect to the Au_4^+Ar cluster. The introduction of Pd allows for intraband sp-sp transitions, which occur between elements. Peak A of Figure 3c corresponds to an Au to Pd transition, with elemental contributions of 95/5/0 in the initial state, and 20/79/1 in the final state (Au/Pd/Ar percentages). Peak B, in contrast, is a Pd to Au transition, with elemental contributions of 34/65/1 and 85/15/0 in the initial and final states, respectively.

4.2.3 Au_5^+Ar and $PdAu_4^+Ar$ clusters

For the Pd-doped cluster $PdAu_4Ar^+$, peak A at 3.57 eV (Figure 4b) consists of Au(sd) to Pd(p) interatomic charge transfer character. The bands of higher energy transitions in the range 3.8-4.3 eV also have primarily Au-Pd character. Charge transfer transitions therefore occur in the same interelemental manner, and involve the same orbitals as for the 4-atom metal clusters. However, it should be noted that for the global minimum cluster structure found for $PdAu_4Ar^+$, the total static charge transfer from Au to Pd, from Löwdin analysis, is found to be less extensive than for the smaller clusters. The MO pair which contributes most to the (lowest energy) transition at 3.85 eV in Au_5^+Ar has a weight of 93% Au and 7% Ar in the initial state, and 73% Au, 27% Ar in the final state. The greatest atomic orbital weights for this peak are, however, located on Au atoms, with Au d_{xz}/d_{yz} and Au sp the largest contributors in the initial and final states, respectively. For the higher energy peaks at 4.08 and 4.32 eV, the MO pairs involve Au d orbitals as the major component of the initial state, and Au sp orbitals in the final state. The excitation with large oscillator strength at 4.60 eV has a slightly different character, consisting of Au sp (85% on Au) to Au s (95% on Au) transition.

4.4. Conclusion

- 1 [48] A. M. Rappe, K. M. Rabe, E. Kaxiras and J. D. Joannopoulos, *Phys. Rev. B* **1990**, *41*,
2
3 1227.
4
5 [49] M. Valiev, E. Bylaska, N. Govind, K. Kowalski, T. Straatsma, H. Van Dam, D. Wang, J.
6
7 Nieplocha, E. Apra, T. Windus and W. de Jong, *Comput. Phys. Commun.* **2010**, *181*, 1477.
8
9 [50] F. Weigend and R. Ahlrichs, *Phys. Chem. Chem. Phys.* **2005**, *7*, 3297.
10
11 [51] O. A. Vydrov and G. E. Scuseria, *J. Chem. Phys.* **2006**, *125*, 234109.
12
13 [52] M. A. Rohrdanz, K. M. Martins and J. M. Herbert, *J. Chem. Phys.* **2009**, *130*, 054112.
14
15 [53] L. Skripnikov, Chemissian, *A Computer Program to Analyse and Visualise Quantum-*
16
17 *Chemical Calculations*, **2012**.
18
19 [54] J. U. Andersen, E. Bonderup, K. Hansen, P. Hvelplund, B. Liu, U. V. Pedersen and S.
20
21 Tomita, *Eur. Phys. J. D* **2003**, *24*, 191.
22
23 [55] A. Shayeghi, R.L. Johnston, D.M. Rayner, R. Schäfer and A. Fielicke, *Angew. Chem. Int.*
24
25 *Ed.* **2015**, *54*, 10675.
26
27 [56] B. Kalita and R. C. Deka, *J. Chem. Phys.* **2007**, *127*, 244306.
28
29 [57] S. Heiles, A. J. Logsdail, R. Schäfer and R. L. Johnston, *Nanoscale* **2012**, *4*, 1109.
30
31 [58] S. Zhao, X. Tian, J. Liu, Y. Ren and J. Wang, *Comp. Theor. Chem.* **2015**, *1055*, 1.
32
33 [59] S. Peng, L. Gan, R. Tian and Y. Zhao, *Comp. Theor. Chem.* **2011**, *977*, 62.
34
35 [60] S. Ögüt, J. C. Idrobo, J. Jellinek, J. Wang, *J. Cluster Sci.* **2006**, *17*, 609.
36
37 [61] University of Birmingham, Birmingham Environment for Academic Research,
38
39 <http://www.bear.bham.ac.uk/bluebear> (accessed 01, 2016).
40
41
42
43
44
45
46
47
48
49
50
51
52
53
54
55
56
57
58
59
60
61
62
63
64
65

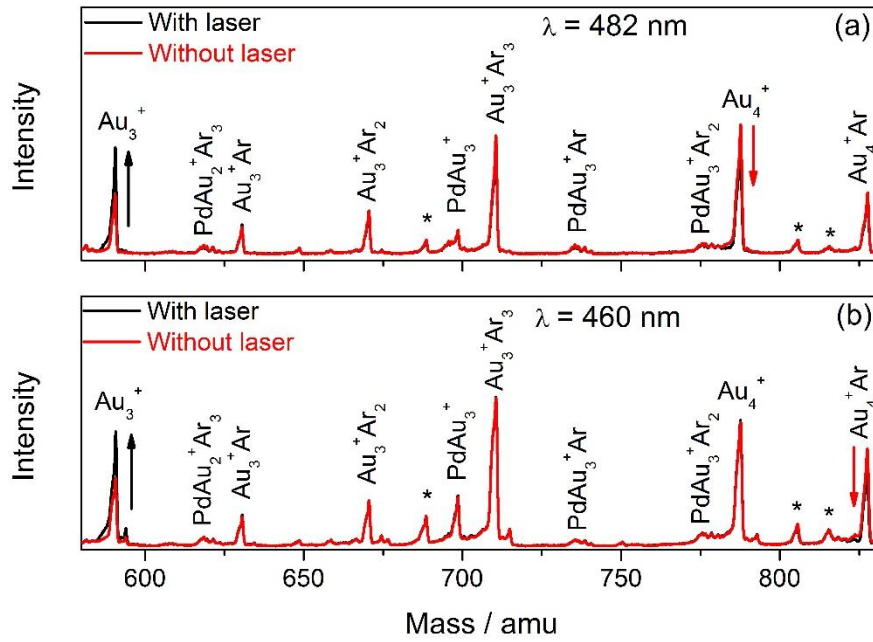


Figure 1. Mass spectra with (black) and without (red) laser excitation at (a) 480 nm and (b) 460 nm. The decrease in signal for Au_4^+ at 482 nm and for Au_4^+Ar at 460 nm (indicated by an arrow) implies laser induced fragmentation of these clusters. In contrast, the increase in Au_3^+ signal shows that this cluster is the fragmentation channel of Au_4^+ (at 482 nm). The similar increase of Au_3^+ at $\lambda=460$ nm proves that Au_3^+ is also a product ion of the fragmentation of Au_4^+Ar . The * correspond to oxygen contaminated clusters.

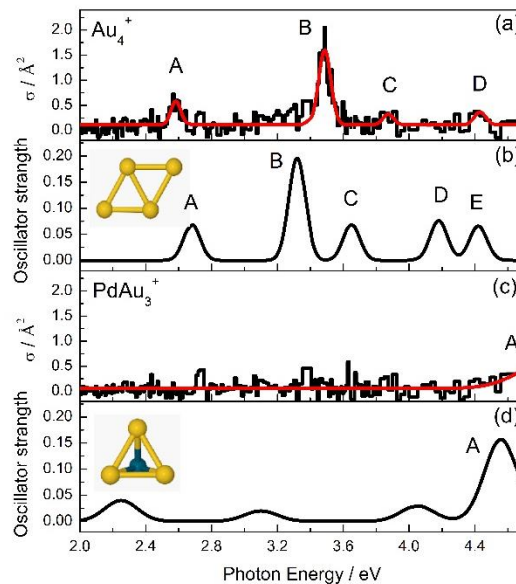


Figure 2. Comparison of experimental photodissociation ((a) and (c)) and calculated electronic excitation ((b) and (d)) spectra of the lowest energy isomers for Au_4^+ and PdAu_3^+ . **Black step lines** represent the experimental data while red solid lines are multi-Gaussian fits. Absorption cross sections are obtained by Equation 1 from measured photodepletions. The corresponding lowest energy isomers are displayed as insets in the figure with Au atoms shown in yellow and Pd in blue.

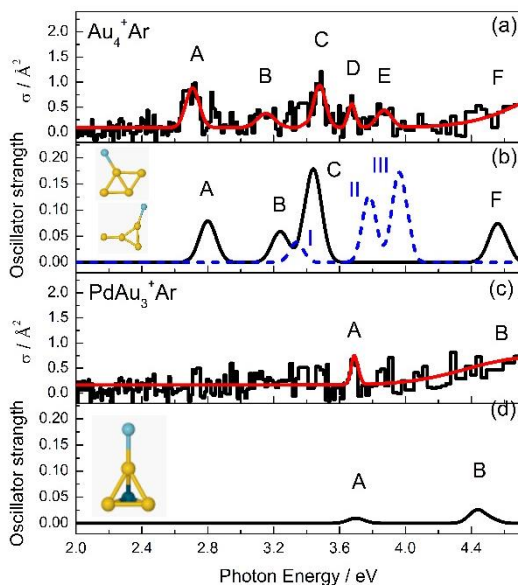


Figure 3. Comparison of experimental photodissociation ((a) and (c)) and calculated electronic excitation ((b) and (d)) spectra of the lowest energy isomers for Au_4^+Ar and PdAu_3^+Ar . **Black step lines** represent the experimental data while red solid lines are multi-Gaussian fits. Absorption cross sections are obtained by Equation 1 from measured photodepletions. The corresponding lowest energy isomers are displayed as insets in the figure with Au atoms shown in yellow, Pd in blue and Ar in sky-blue. **In (b) the Y-shaped isomer of Au_4^+Ar , 0.11 eV higher in energy than the global minimum, is shown by dashed blue line.**

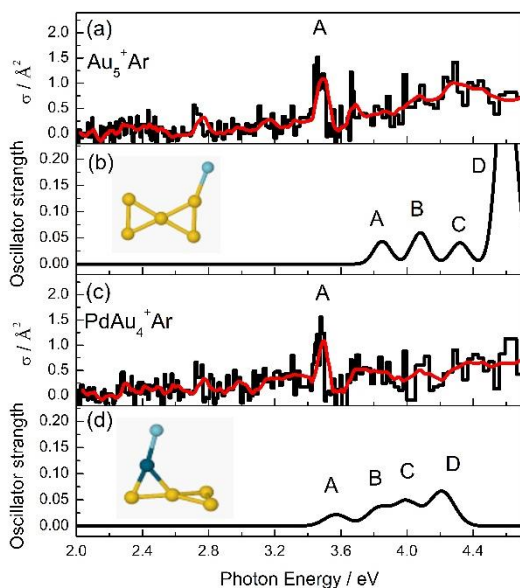


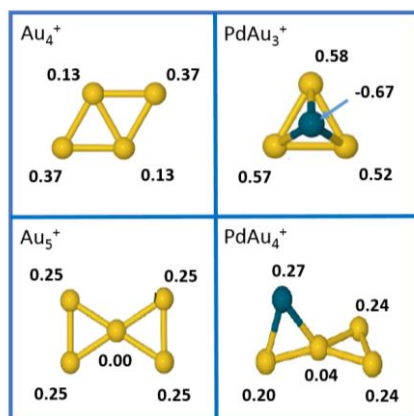
Figure 4. Comparison between experimental photodissociation and calculated electronic excitation spectra of the lowest energy isomer for Au_5^+Ar and PdAu_4^+Ar . In (a) and (c) experimental spectra are presented for Au_5^+Ar and PdAu_4^+Ar , respectively. **Black step lines**

2222222222222222224222222

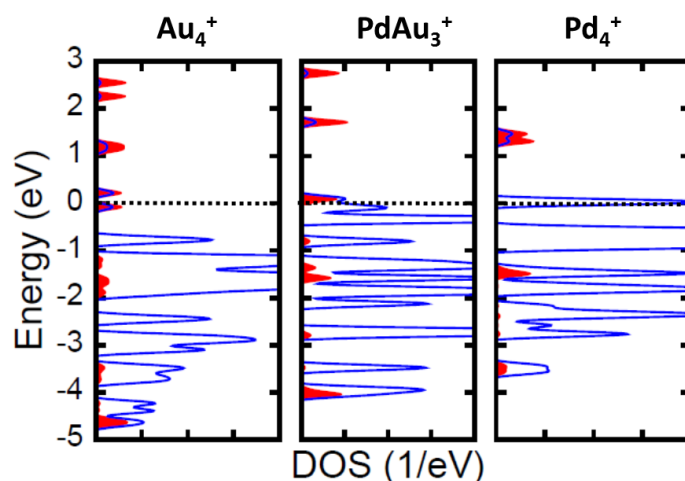
Particle

Submitted to & Particle Systems Characterization

1 represent the experimental data while solid lines an averaged curve of 3-adjacent points.
2 Absorption cross sections are obtained by Equation 1 from the measured photodepletions. In
3 addition, (b) and (d) show calculated spectra for Au_5^+Ar and PdAu_4^+Ar , respectively. The
4 corresponding lowest energy isomers are displayed as insets in the figure with Au atoms
5 shown in yellow, Pd in blue and Ar in sky-blue.
6
7
8
9
10
11
12



13
14
15
16
17
18
19
20
21
22
23
24
25
26
27
28 **Figure 5.** Calculated atomic charges of the lowest energy structures of Au_n^+ and PdAu_{n-1}^+ (n
29 $= 4, 5$) using the Löwdin scheme. Au atoms are shown in yellow and Pd in blue.
30
31
32
33
34
35
36
37
38



56 **Figure 6.** Projected density of states for Au_4^+ , PdAu_3^+ and Pd_4^+ , calculated at the PBE level of
57 theory. Electron density is projected onto s (filled red lines) and d (blue lines) atomic orbitals,
58 and presented relative to the Fermi energy (dashed black line).
59
60
61
62
63
64
65

Table 1. Most favorable fragmentation channels and their corresponding dissociation energies obtained by DFT calculations.

Mother species	Fragments	Dissociation energy [eV]
Au ₄ ⁺	Au ₃ ⁺ + Au	1.33
PdAu ₃ ⁺	PdAu ₂ ⁺ + Au	2.25
Au ₄ ⁺ Ar	Au ₄ ⁺ + Ar	0.21
Au ₄ ⁺ Ar	Au ₃ ⁺ + Au + Ar	1.54
PdAu ₃ ⁺ Ar	PdAu ₃ ⁺ + Ar	0.23
PdAu ₃ ⁺ Ar	PdAu ₂ ⁺ + Pd + Ar	2.58
Au ₅ ⁺	Au ₃ ⁺ + Au ₂	2.17
PdAu ₄ ⁺	PdAu ₃ ⁺ + Au	1.64
Au ₅ ⁺ Ar	Au ₅ ⁺ + Ar	0.21
PdAu ₄ ⁺ Ar	PdAu ₃ ⁺ + Ar	0.23

Table 2. Peak positions and oscillator strengths of the absorption bands for the studied clusters. Peaks are labelled according to Figure 1, 2 and 3. Experimental oscillator strengths are calculated by $f = 0.91103 \int d(E)dE$ and the Gaussian fits of the experimental data.^[19,21]

	Peak	Position (eV)		Oscillator strength	
		Exp.	Theory	Exp.	Theory
Au ₄ ⁺	A	2.58 ± 0.01	2.68	0.033 ± 0.006	0.070
	B	3.49 ± 0.01	3.32	0.125 ± 0.007	0.200
	C	3.87 ± 0.02	3.65	0.016 ± 0.009	0.070
	D	4.43 ± 0.02	4.18	0.011 ± 0.009	0.080
	E		4.42		0.080
PdAu ₃ ⁺	A	> 4.70	4.56	> 0.080	0.170
Au ₄ ⁺ Ar	A	2.71 ± 0.01	2.80	0.074 ± 0.009	0.080
	B	3.15 ± 0.02	3.24	0.034 ± 0.012	0.060
	C	3.48 ± 0.01	3.44	0.070 ± 0.009	0.180
	D	3.67 ± 0.01		0.023 ± 0.009	
	E	3.87 ± 0.02		0.035 ± 0.013	
	F	> 4.70	4.56	> 0.070	0.080
PdAu ₃ ⁺ Ar	A	3.69 ± 0.02	3.70	0.028 ± 0.005	0.009
	B	> 4.70	4.44	> 0.100	0.026
Au ₅ ⁺ Ar	A	3.46 ± 0.01	3.85	0.089 ± 0.010	0.045
	B		4.08		0.063
	C		4.32		0.043

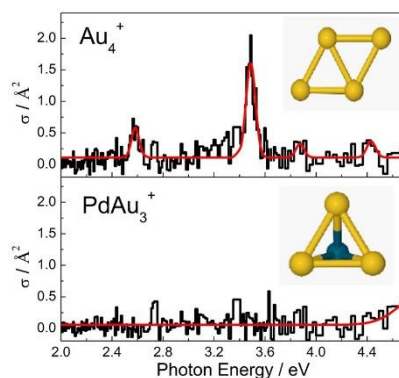
	D		4.60		0.467
PdAu ₄ ⁺ Ar	A	3.48 ± 0.03	3.57	0.077 ± 0.009	0.022
	B		3.83		0.035
	C		4.00		0.048
	D		4.24		0.020

The effect of a single Pd dopant atom in the optical absorption of the small gas phase Au₄⁺ and Au₅⁺ clusters is studied by a combination of photodissociation spectroscopy and density functional theory calculation. A quenching of most absorption bands is observed and attributed to charge transfers and structural changes induced by the Pd dopant atom.

Optical absorption

V. Kaydashev, P. Ferrari, C. Heard, E. Janssens*, R. L. Johnston, and P. Lievens

Optical absorption of small palladium doped gold clusters



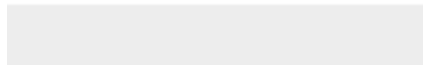
Copyright WILEY-VCH Verlag GmbH & Co. KGaA, 69469 Weinheim, Germany, 2013.



Click here to access/download

Supporting Information

SupportinginformationFinal_Revision.docx

















Click here to access/download
Production Data
ToC.tif

